daf-16: An HNF-3/forkhead Family Member That Can Function to Double the Life-Span of *Caenorhabditis elegans*

Kui Lin, Jennie B. Dorman,* Aylin Rodan, Cynthia Kenyon

The wild-type *Caenorhabditis elegans* nematode ages rapidly, undergoing development, senescence, and death in less than 3 weeks. In contrast, mutants with reduced activity of the gene *daf-2,* a homolog of the insulin and insulin-like growth factor receptors, age more slowly than normal and live more than twice as long. These mutants are active and fully fertile and have normal metabolic rates. The life-span extension caused by *daf-2* mutations requires the activity of the gene *daf-16. daf-16* appears to play a unique role in life-span regulation and encodes a member of the hepatocyte nuclear factor 3 (HNF-3)/forkhead family of transcriptional regulators. In humans, insulin down-regulates the expression of certain genes by antagonizing the activity of HNF-3, raising the possibility that aspects of this regulatory system have been conserved.

The identification of genes that regulate aging (*1*) is an important breakthrough because it provides a means of investigating this fundamental but poorly understood process. The nematode *Caenorhabditis elegans* has a very rapid rate of aging (*2*), which is due in part to the activity of the gene *daf-2*. Mutations that reduce the activity of *daf-2*, a homolog of the insulin and insulin-like growth factor (IGF) receptors (*3*), can slow the rate of aging and more than double the life-span of the animal (*4*) without substantially affecting its activity or fertility (*4–6*). The life-span extension caused by *daf-2* mutations requires the gene *daf-16* (*4*).

In addition to regulating the rate of aging, *daf-2* and *daf-16* also regulate the decision to enter diapause (the dauer phase) (*7–10*). When food is limited, young animals become dauers instead of developing to adulthood (*9*). The dauer is a resilient, long-lived, juvenile form that remains small and reproductively immature. Wild-type *daf-2* activity promotes growth to adulthood and prevents dauer formation. Unlike partial loss of *daf-2* function, which specifically affects life-span, more severe loss of *daf-2* function causes the animals to become dauers even in the presence of food (*7–11*). Thus, *daf-2*(+) has two functions: It promotes growth to adulthood, and it shortens the life-spans of adult animals (*12*). In addition to its role in life-span extension, the wild-type *daf-16* gene is also required for dauer formation in both wild-type and *daf-2*(−) animals (*7–11*). Thus, *daf-16* also has two functions: Under dauer-inducing conditions, it promotes dauer formation, and, under conditions that do not induce dauer formation, it allows fertile adults carrying weak *daf-2* mutations to remain active for a much longer period and to live twice as long as normal (*4*).

Because so few genes are known to regulate aging in any organism, we asked how many other genes were likely to have functions similar to that of *daf-16*. To do this, we carried out a genetic screen for additional *daf-16*–like mutants. *daf-16* mutations, as well as mutations in functionally related genes required for both dauer formation and life-span, can be isolated easily as suppressors of *daf-2* mutations (*7–9*). We mutagenized *daf-2(e1370)* hermaphrodites with trimethylpsoralen followed by ultraviolet (UV) irradiation, which causes both point mutations and deletions (*13*), and screened their descendants for rare individuals that did not become dauers but instead grew to adulthood. We found 24 independent *daf-2* suppressors, all of which proved to be new alleles of *daf-16* (*14*). This result suggests that there are not a large number of genes like *daf-16*. Instead, any genes that act along with, or downstream of, *daf-16* to initiate dauer formation are likely to affect only certain aspects of dauer formation or else are functionally redundant or essential (*15*). Thus, *daf-16* provides a unique starting point for understanding how aging can be regulated.

We cloned *daf-16* by transposon tagging (*16, 17*). We isolated a *daf-16::Tc1* insertion mutation, *mu147*, by looking for *daf-2* suppressors in a *daf-2; mut-6* strain, in which the transposon Tc1 is active (Fig. 1, A and B) (*16*). We then cloned the genomic DNA containing this Tc1 element and used sequences flanking Tc1 as a probe in Southern blot analysis of DNA isolated from our trimethylpsoralen-induced *daf-16* mutants. In five mutants, we found changes in the mobility of the restriction fragments that hybridized to the probe (Fig. 1C).

The Tc1-tagged DNA was sequenced and found to be present on the cosmid R13H8, which was sequenced by the C. *elegans* sequencing project (*18*). We obtained the corresponding cDNA sequences by performing

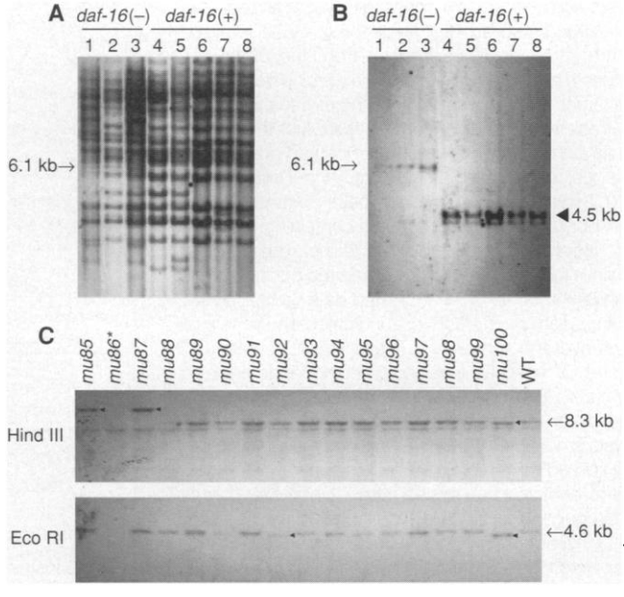

Fig. 1. Identification of a *daf-16::Tc1* insertion mutant. (**A** and **B**) Cosegregation of a Tc1-containing fragment with the *daf-16(mu147)* mutation. In (A), Xba I–digested genomic DNA was probed with Tc1. The arrow points to the 6.1-kb fragment, which was present in 20 of 20 *daf-16*(−) recombinants (three are shown in lanes 1 to 3) but absent in 15 of 15 *daf-16*(+) recombinants (five are shown in lanes 4 to 8) and also absent in the wild-type strain N2 (not shown) (*16*). In (B), the same filter was probed with genomic sequences flanking this Tc1 element. All *daf-16*(+) recombinants as well as N2 (not shown) contained a single 4.5-kb hybridizing fragment (arrowhead); all *daf-16*(−) recombinants lacked this band and instead contained a band 1.6 kb larger (arrow; Tc1 is 1.6 kb). (**C**) Genomic DNA from the trimethylpsoralen-induced mutants was probed with the sequence flanking Tc1. Five mutants exhibited changes in the mobility of these restriction fragments. Arrowheads indicate mobility shifts; the lack of a hybridizing band in *mu86* is indicated by an asterisk. WT, wild type.

Department of Biochemistry and Biophysics, University of California, San Francisco, CA 94143–0554, USA.

*Present address: Molecular and Cellular Biology Program, University of Washington, Seattle, WA 98195–7275, USA.

reverse transcription polymerase chain reaction (RT-PCR) and by analyzing clones from the *C. elegans* expressed sequence tag (EST) database (*19*) (Fig. 2). Both methods identified a cDNA species consisting of 10 exons and containing a single open reading frame predicted to encode a protein of 510 amino acids (Fig. 2, A and B).

The sequence of this gene was found to be homologous to members of the HNF-3/forkhead family, a large class of transcription factors characterized by the presence of a forkhead domain, an ~110–amino acid domain that forms a winged helix structure and mediates DNA binding (*20*). Members of this family have many different roles in embryogenesis, tumorigenesis, and differentiation and have been found to function at downstream positions in several types of signaling pathways (*20*), including insulin pathways (described below). The *daf-16* forkhead domain was most similar to those of human FKHR and AFX proteins (67% and 64% identity, respectively), both of which were identified as human oncogenic fusion proteins (*20*) (Fig. 3). As with other HNF-3/forkhead family members, little similarity was present outside of this region.

We verified that this gene was *daf-16* by identifying sequence changes in the Tc1 insertion mutant, two previously identified *daf-16* mutants, *m26* and *m27*, and eight trimethylpsoralen-induced mutations that

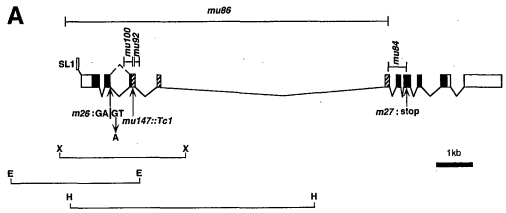

Fig. 2. *daf-16* encodes an HNF-3–forkhead homolog. (**A**) The structure of the *daf-16* gene. The genomic DNA sequence spans at least 14 kb and contains 10 exons (boxes). The predicted coding regions are filled in black, and the regions homologous to the forkhead–winged helix domain are hatched. The changes in seven *daf-16* mutations, *m26*, *m27*, *mu147*, *mu100*, *mu92*, *mu86*, and *mu84*, are shown [four additional mutations (*mu85*, *mu87*, *mu89*, and *mu91*) contained deletions that were detected by Southern blot analysis or PCR but were not sequenced]. *m26* harbors a single GC to AT transition at the 5′ splice junction (indicated by a vertical bar) of intron 2. The positions of the Xba I (X) fragment containing the Tc1 insertion in *mu147* and those of the Eco R1 (E) and Hind III (H) restriction fragments that were altered in the *daf-16* mutants (Fig. 1C) are shown. The use of two alternative 3′ splice sites for intron 2 is indicated by solid and dashed lines. (**B**) The *daf-16* cDNA and predicted amino acid sequence (GenBank accession number AF032112). The *daf-16* message we analyzed was trans-spliced with an SL1 leader (*33*). Open triangles indicate intron positions inferred from the cDNA sequences. The six base pairs that are missing from one of the alternatively spliced forms are boxed; the predicted amino acid residue at position 121 is a Glu in the shorter (508 amino acids) form (not shown) instead of an Asp in the longer (510 amino acid) form. A polyadenylation [poly(A)] signal is found 11 base pairs upstream of the site of poly(A) in RT-PCR products containing the longest 3′ untranslated region (bold underline). The forkhead domain is indicated by brackets, and the position of the Tc1 insertion in *mu147* is indicated by a vertical arrow. Primers used in RT-PCR are indicated by horizontal arrows over the sequences. The 3′ RACE primers (Q_T, Q_O, and Q_I) used for isolating 3′ cDNA ends are also shown (*34*). The *m27* GC to AT amber mutation is indicated by an asterisk over the site. The *m26* mRNA analysis is not shown, but RT-PCR detected two abnormally spliced mRNA species from this mutant. The major form contained unspliced intron 2 and therefore is 645 bp longer than the wild-type longer form; the minor form (~10% of the product) lacked the last two nucleotides of exon 2 because of the use of a noncanonical 5′ splice site GA instead of GU. Both forms predicted early stop codons shortly after exon 2. A downstream in-frame ATG was found in both cases, however,with the potential to encode a 400–amino acid protein in the major form bearing an altered NH_2-terminal region and the intact forkhead domain and COOH-terminal region as well as a 353–amino acid protein in the minor form with the NH_2-terminal region (including part of the forkhead domain) truncated. No correctly spliced form was detected in the *m26* mRNA. Also not shown is the *mu100* mRNA analysis,which resulted in an abnormally spliced mRNA bearing an early stop codon predicted to remove most of the forkhead domain and all COOH-terminal regions. Abbreviations for the amino acid residues are as follows: A, Ala; C, Cys; D, Asp; E, Glu; F, Phe; G, Gly; H, His; I, Ile; K, Lys; L, Leu; M, Met; N, Asn; P, Pro; Q, Gln; R, Arg; S, Ser; T, Thr; V, Val; W, Trp; and Y, Tyr.

we analyzed (Fig. 2, A and B). Several mutations affected the conserved forkhead domain and were predicted to prevent DNA binding. The *mu147* Tc1 insertion was located within the forkhead domain, *m26* altered a splice donor sequence upstream of the forkhead domain, *mu84* deleted part of the forkhead domain and some of the COOH-terminal region, and *mu100* and *mu92* both affected splice junctions of exon 3, which encodes part of the forkhead domain. In contrast, one mutation, *m27*, created a stop codon ~100 amino acids COOH-terminal to the forkhead domain. Semiquantitative RT-PCR analysis indicated that this mutation did not affect *daf-16* mRNA levels, implying that it may encode a truncated DAF-16 protein containing the DNA binding domain but lacking the COOH-terminal region (*21*). This finding suggests that sequences downstream of the forkhead domain may be required for DAF-16 function. The COOH-terminal region of the forkhead family member FAST-1 has been found to mediate protein-protein interactions (*22*); whether a similar function exists for this region of DAF-16 awaits further analysis.

The dauer-defective phenotype of *daf-16* is semidominant (*8*); therefore, it was particularly important to confirm that the Daf-16 mutant phenotype resulted from reduced rather than altered or novel gene activity. Our findings indicated that this is the case, because most of these mutations would be predicted to reduce or eliminate *daf-16* activity. To determine whether any of these mutations were null alleles, we analyzed mRNA expression in the mutants. For the majority of alleles, it was not possible to completely rule out the possibility that residual *daf-16* function might still exist (Fig. 2B). However, one mutation, *mu86*, was likely a null allele. This mutation was a large deletion that removed most of the coding sequence, including all of the forkhead domain. This mutant, like all other known *daf-16* alleles, grew to become an active, fertile adult. This finding suggests that *daf-16* functions primarily to regulate life-span and dauer formation and does not have essential activities.

The finding that *daf-16* encodes an HNF-3/forkhead family member is important because it implies that mutations in the *daf-2* insulin/IGF receptor homolog exert their effects not simply by changing the activities of preexisting enzymes (*23*) but instead by initiating a new genetic regulatory program that extends youthfulness and postpones death. There are several intriguing parallels between this *C. elegans* pathway and the human insulin/IGF pathways (*3*). In humans, insulin and IFG regulate food utilization pathways and promote growth (*23*). Similarly, *daf-2* activity promotes growth to adulthood when food is abundant; conversely, lack of *daf-2* activity maintains the dauer state, in which the animals use stored food sources. In animals that lack *daf-16* activity, *daf-2* mutations have little or no effect, which raises the possibility that the primary role of *daf-2* is to prevent *daf-16* function (*7–9*). In humans, insulin appears to mediate some of its effects by blocking the activity of HNF-3 (*24*). Of four insulin-repressed genes that have been studied extensively, three, phosphoenolpyruvate carboxykinase, tyrosine amino transferase, and IGF binding protein–1, appear to be up-regulated by HNF-3 in the absence of insulin. Each gene contains a similar insulin-response sequence (IRS) that can act as a binding site for HNF-3 and that is required for repression by insulin. It has been proposed that insulin signaling acts by preventing HNF-3 from binding to the IRS (*24*, *25*).

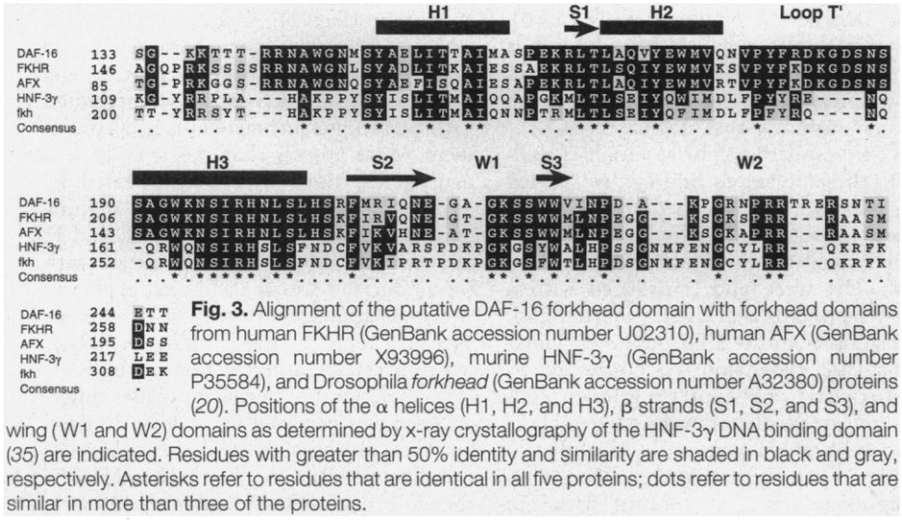

Fig. 3. Alignment of the putative DAF-16 forkhead domain with forkhead domains from human FKHR (GenBank accession number U02310), human AFX (GenBank accession number X93996), murine HNF-3γ (GenBank accession number P35584), and Drosophila *forkhead* (GenBank accession number A32380) proteins (*20*). Positions of the α helices (H1, H2, and H3), β strands (S1, S2, and S3), and wing (W1 and W2) domains as determined by x-ray crystallography of the HNF-3γ DNA binding domain (*35*) are indicated. Residues with greater than 50% identity and similarity are shaded in black and gray, respectively. Asterisks refer to residues that are identical in all five proteins; dots refer to residues that are similar in more than three of the proteins.

So far, little is known about how *daf-2* might affect *daf-16* activity in *C. elegans*. *daf-2* may exert its effects by activating the phosphatidylinositol 3-kinase *age-1*, because mutations in this gene also extend life-span in a *daf-16*–dependent fashion (*5*, *26–30*).

In vertebrates, caloric restriction, which affects insulin levels, has an effect analogous to that of weak *daf-2* mutations: It also extends life-span without decreasing the rate of metabolism (*31*). Thus, life-span in both *C. elegans* and vertebrates may be regulated by an evolutionarily conserved mechanism involving a forkhead homolog that promotes longevity when food is scarce and an insulin family member that counteracts it. In addition, it is possible that the different aging rates of different individuals within a species, as well as the markedly different aging rates exhibited by members of different species, are due in part to intrinsic differences in the resting levels of this signaling pathway.

Note added in proof: Working independently, Ogg *et al.* have also cloned and molecularly analyzed *daf-16* (*36*).

REFERENCES AND NOTES

1. S. M. Jazwinski, *Science* **273**, 54 (1996); T. Smeal and L. Guarente, *Curr. Opin. Genet. Dev.* **7**, 281 (1997); C. Kenyon, *Cell* **84**, 501 (1996).
2. C. Kenyon, in *C. elegans II*, D. R. Riddle, T. Blumenthal, B. Meyer, J. Priess, Eds. (Cold Spring Harbor Laboratory Press, Cold Spring Harbor, NY, 1997), pp. 791–814.
3. K. D. Kimura, H. A. Tissenbaum, Y. Liu, G. Ruvkun, *Science* **277**, 942 (1997).
4. C. Kenyon, J. Chang, E. Gensch, A. Rudner, R. Tabtiang, *Nature* **366**, 461 (1993).
5. P. L. Larsen, P. S. Albert, D. L. Riddle, *Genetics* **139**, 1567 (1995).
6. J. R. Vanfleteren and A. DeVreese, *FASEB J.* **9**, 1355 (1995); *J. Exp. Zool.* **274**, 93 (1996).
7. D. L. Riddle, M. M. Swanson, P. S. Albert, *Nature* **290**, 668 (1981).
8. S. Gottlieb and G. Ruvkun, *Genetics* **137**, 107 (1994).
9. D. Riddle and P. S. Albert, in *C. elegans II*, D. R. Riddle, T. Blumenthal, B. Meyer, J. Priess, Eds. (Cold Spring Harbor Laboratory Press, Cold Spring Harbor, NY, 1997), pp. 739–768.
10. J. J. Vowels and J. H. Thomas, *Genetics* **130**, 105 (1992).
11. The process of dauer formation is facilitated by high temperature; therefore, many *daf-2* mutations induce dauer formation at high but not low temperature. At low temperature (or when shifted to high temperature as young adults, past the dauer decision point), these *daf-2* mutants become long-lived adults (*4*).
12. Because dauers are long-lived, one explanation for these two roles is that weak *daf-2* mutations allow adults to express only one feature of the dauer, namely its slow rate of aging.
13. M. D. Yandell, L. G. Edgar, W. B. Wood, *Proc. Natl. Acad. Sci. U.S.A.* **91**, 1381 (1994).
14. *daf-2(e1370ts)* L4-stage animals were mutagenized with trimethylpsoralen followed by UV irradiation (*13*), and F_2 progeny were screened for their ability to grow to adulthood at 25°C. Twenty-four independent *daf-2* suppressers, *mu84* to *mu107*, were isolated, all of which proved to be *daf-16* alleles. We performed complementation tests by crossing *daf-16(m26); daf-2(e1370); him-5(e1490)* males with

sup; daf-2(e1370) hermaphrodites at the nonpermissive temperature and examining cross progeny for dauer formation. The descendants of the cross progeny were also examined to ensure that the mutations were not unlinked, noncomplementing mutations. We also mapped many of the mutations by testing for linkage with *unc-29,* which maps near *daf-16,* or else with *daf-16*–linked restriction fragment length polymorphisms using PCR (*32*).

15. One such gene may be *daf-18.* This gene has been identified by a single mutation that suppresses both dauer formation and the life-span extension of *daf-2* mutants (*7*, *10*, *28*). However, many *daf-18* individuals show severe morphological abnormalities, suggesting that this gene has other, possibly essential, functions (*28*). The fact that we did not find any *daf-18* alleles supports this hypothesis. In addition, we note that because we screened F_2 progeny of mutagenized animals, we would have missed mutants that were maternally rescued.
16. We first attempted to clone *daf-16* by positional mapping but found that the gene was located in a gap in the physical map between cosmids AE7 and ZK39. To isolate *daf-16::Tc1* insertion mutants, we screened *daf-2(sa189); mut-6* animals for spontaneous mutants that did not become dauers when cultured at 20°C. One mutant, *mu147,* also suppressed dauer formation at 25°C. This mutation failed to complement *daf-16(m26)* and was closely linked to *unc-29*, which maps near *daf-16. mu147* was subsequently crossed to either *unc-29(e1072); daf-2(e1370); him-5(e1490)* or *daf-2(e1370); him-5(e1490)* mutants, and homozygous Daf-16(−) and Daf-16(+) recombinants were obtained. Genomic DNA was prepared from these recombinants and analyzed by Southern blot hybridization with the 1.6-kb Tc1 sequence as probe. A 6.1-kb Tc1-hybridizing fragment was detected in the Xba I–digested genomic DNA, which was present in 20 of 20 *daf-16*(−) recombinants but absent in 15 of 15 *daf-16*(+) recombinants and also absent in the wild-type strain (N2). DNA from the corresponding region was then extracted from agarose gels and circularized by self-ligation. An inverse PCR strategy was used to identify a Tc1-containing fragment with the expected size of 5.1 kb. The Tc1-specific primers used for inverse PCR were 5′-CCTTGTTCGAAGCCAGCTACAATGGC-3′ and 5′-TGATCGACTCGATGCCACGTCGTTGT-3′. The 5.1-kb PCR product was cloned into the pGEM-T vector (Promega, Madison, WI), and the 0.6-kb flanking Tc1 sequence was removed by digestion with Eco RV. The remaining sequence was then used as a probe in subsequent experiments.
17. R. H. A. Plasterk and H. G. A. M. van Luenen, in *C. elegans II,* D. R. Riddle, T. Blumenthal, B. Meyer, J. Priess, Eds. (Cold Spring Harbor Laboratory Press, Cold Spring Harbor, NY, 1997), pp. 97–116.
18. J. Sulston *et al., Nature* **356**, 37 (1992); R. Wilson *et al., ibid.* **368**, 32 (1994).
19. RT-PCR was performed with an SL1 primer to obtain the 5′ end of the gene and with Q_T, Q_O, and Q_I to obtain the 3′ end by rapid amplification of cDNA ends (RACE), as well as with several internal primers (positioned as shown in Fig. 2B). In addition, blast searches with sequences contained on R13H8 identified three cDNA clones (yk13f11, yk31f10, and yk32f8) in a *C. elegans* EST database. Complete sequences of clones yk13f11 and yk31f10 were then obtained, and both contained the longer form of the transcripts, whereas the majority of the RT-PCR products (with mixed-stage RNA preparations) contained the shorter form (see Fig. 2). In addition, the longer spliced form was also detected by RT-PCR.
20. E. Kaufmann and W. Knochel, *Mech. Dev.* **57**, 3 (1996).
21. K. Lin, J. Dorman, A. Rodan, C. Kenyon, data not shown.
22. X. Chen *et al., Nature* **389**, 85 (1997).
23. P. Flakoll, M. G. Carlson, A. Cherrington, in *Diabetes Mellitus,* D. LeRoith, S. I. Taylor, J. M. Olefsky, Eds. (Lippincott-Raven, Philadelphia, PA, 1996), pp. 121–131.
24. R. M. O'Brien and D. K. Granner, in *ibid.*, pp. 234–241.
25. R. M. O'Brien *et al., Mol. Cell. Biol.* **15**, 1747 (1995).
26. D. B. Friedman and T. E. Johnson, *Genetics* **118**, 75 (1988).
27. J. Z. Morris, H. A. Tissenbaum, G. Ruvkun, *Nature* **382**, 536 (1996).
28. J. B. Dorman, B. Albinder, T. Shroyer, C. Kenyon, *Genetics* **141**, 1399 (1995).
29. S. Murakami and T. E. Johnson, *ibid.* **143**, 1207 (1996).
30. Neither gain of function (*n1046)* nor dominant negative (*sy100)* mutations in the *C. elegans* Ras homolog *let-60* affected *C. elegans* life-span (because these mutants cannot lay eggs, their gonads were ablated to prevent premature death from internal hatching). In addition, *let-60(n1046gf)* did not suppress the dauer-constitutive phenotype of *daf-2(e1370)* (J. Apfeld and C. Kenyon, unpublished data).
31. C. E. Finch, *Longevity, Senescence, and the Genome* (Univ. of Chicago Press, Chicago, IL, 1990).
32. B. D. Williams *et al., Genetics* **131**, 609 (1992).
33. M. Krause and D. Hirsh, *Cell* **49**, 753 (1987).
34. M. A. Frohman, *Methods Enzymol.* **28**, 341 (1993).
35. K. L. Clark, E. D. Halay, E. Lai, S. K. Burley, *Nature* **364**, 412 (1993).
36. S. Ogg *et al., ibid.* **389**, 994 (1997).
37. We thank N. Ahmada for technical assistance with positional mapping (*16*); B. Albinder, M. Macrae, J. Reiter, T. Wang, D. Eisenstadt, I. Reichardt, and J. Blumstein for helping to isolate and characterize trimethylpsoralen- and Tc1-induced *daf-16* mutants; J. Apfeld in our laboratory for investigating the role of Ras in the *daf-2* signaling pathways (*30*); members of the Kenyon lab for discussions and comments on the manuscript; and Y. Kohara for sending us EST clones of *daf-16*. Supported by NIH grant AG11816. C.K. is the Herbert Boyer Professor of Biochemistry and Biophysics.

19 August 1997; accepted 15 October 1997

TECHNICAL COMMENTS

Immune Response and Myoblasts That Express Fas Ligand

Henry T. Lau *et al.* (*1*) report that syngeneic myoblasts that expressed Fas ligand (FasL, CD95L) protected allogeneic islets of Langerhans from immune rejection when cotransplanted under the kidney capsule. The presumed immune privilege conferred by exogenous expression of FasL in this system appeared to be similar to the naturally occurring immune protection described in the anterior chamber of the eye (*2*), in the rodent testis (*3*), and in malignant melanoma (*4*), all of which express endogenous FasL. These studies generated considerable interest in the scientific community because they suggested a method for generating gene- or tissue-specific tolerance with broad applications to organ transplantation. In contrast with these results, others have found that exogenous FasL expression, either by tumor cells or by islets, targeted the cells for rapid destruction by neutrophils (*5*, *6*). Moreover, although a recent report showed a FasL-mediated inhibition of antibody production, it also stated that an inflammatory response was observed (*7*).

To investigate potential variables leading to these divergent findings, we carried out experiments designed to replicate closely those described by Lau *et al.* (*1*). Primary skeletal myoblasts were isolated from C3H mice and transduced with a retroviral vector that directs murine FasL expression from the LTR promoter. Functional FasL expression was confirmed by cytotoxicity to Fas-expressing Jurkat cells (*8*). Unexpectedly, transduced myoblasts underwent rapid apoptosis during differentiation, which suggests that skeletal myoblasts express Fas, in contrast with the findings of Lau *et al.* (*1*). Although shown earlier to occur in postnatal cardiac and skeletal muscle tissues (*9*), Fas expression had, to our knowledge, not been examined in cultured cells. With the use of an antibody to mouse Fas, Jo2 (*10*), we confirmed Fas expression in myoblasts of C3H (Fig. 1) and C57BL/6 strains (*11*).

To avoid Fas/FasL-mediated self-destruction of myoblasts, we generated primary myoblasts from Fas-deficient C57BL/6 lpr mice, the mouse counterpart to human autoimmune lymphoproliferative syndrome (ALPS). When transduced with the FasL vector, lpr myoblasts did not self-destruct on differentiation in vitro. Nontransduced or FasL-transduced lpr myoblasts were injected under the kidney capsule of congenic C57BL/6 mice. Mice were killed 1, 3, 7, 14, and 26 days after transplantation, and their kidneys were removed for histological examination (Fig. 2). Kidneys transplanted with nontransduced myoblasts appeared normal at all time points (Fig. 2, A, C, and E). In contrast, each kidney transplanted with FasL-expressing myoblasts had a prominent white abscess that was abundant in neutrophils; these abscesses appeared by day 1, were pronounced by day 3, and disappeared by day 26 (Fig. 2, B, D, and F, respectively). Moreover, in contrast with the findings of Lau *et al.* (*1*), co-implantation of allogeneic C3H islets of Langerhans with congenic FasL-expressing myoblasts led to accelerated destruction of the islets (Fig. 2G). Untransduced myoblasts differentiated and persisted for at least 26 days, but FasL myoblasts were destroyed by the granulocytic infiltrate (Fig. 2, H and I). It is therefore unclear how Lau *et al.* (*1*) were